

Phase Analysis of the Binary System of Cryolite (Na_3AlF_6) and Sodium Metasilicate (Na_2SiO_3)

by František Šimko*, and Miroslav Boča

Institute of Inorganic Chemistry, Slovak Academy of Sciences, 845 36 Bratislava, Slovak Republic
(phone: 00421-2-59410420; fax: 00421-2-59410444; e-mail: uachsim@savba.sk)

The phase analysis of cryolite (Na_3AlF_6) and sodium metasilicate (Na_2SiO_3) was performed by thermal analysis. The eutectic system with a region of two immiscible substances at a concentration of Na_2SiO_3 between 42.8 and 46.3 mol-% was identified and the eutectic temperature determined to $(886 \pm 2)^\circ\text{C}$. Based on the results of mass-loss measurements, it was assumed that the introduced Na_2SiO_3 reacts with Na_3AlF_6 due to the formation of some nonvolatile stable compounds. The stable reaction products were identified by X-ray diffraction analysis and IR spectroscopy of the spontaneously cooled samples, which established the formation of NaF and stable amorphous aluminosilicate compounds.

1. Introduction. – Aluminium is produced by the electrolysis of alumina dissolved in the cryolite-based melts (the *Hall–Héroult* process). Besides the usual components (cryolite (Na_3AlF_6), AlF_3 , Al_2O_3 , CaF_2), the electrolyte always contains some impurities (especially iron, silicon, and phosphorus compounds), which negatively influence the current efficiency and may decrease the metal quality [1][2]. Because of these reasons, the accumulation of impurities in the electrolyte cells became one of the most serious problems.

In terms of the quantity of impurities, the presence of silicon impurities in the electrolyte is one of the most problematic. These silicon compounds originate from the raw materials and are continuously introduced into the bath by the raw materials feed (alumina, anode materials, and other compounds used for the optimization of the bath composition, mainly AlF_3). Silicon impurities also originate from other sources, namely carbon and refractory lining as well as other parts of the production equipments and tools.

This paper resolves the analysis of the binary system Na_2SiO_3 with cryolite (Na_3AlF_6). Sodium metasilicate (= silicic acid (H_2SiO_3) sodium salt (1:2); Na_2SiO_3) can be one of the stable silicon compounds which are present in the input materials, besides SiO_2 . Up to now, no investigation of Na_2SiO_3 solubility in such a fluoride system was published. Thus, our work is focused on the phase analysis of this system as well as on the specification of possible products by IR spectrometry, X-ray diffraction, and mass-loss measurements.

2. Results and Discussion. – 2.1. *Cryoscopy and Phase Diagram.* The experimentally determined temperatures of the primary and eutectic crystallization of the individual samples of the investigated systems are summarized in *Table 1*.

Table 1. Composition and Temperatures of Primary and Eutectic Crystallization of Melts of the $\text{Na}_3\text{AlF}_6/\text{Na}_2\text{SiO}_3$ System

$x(\text{Na}_2\text{SiO}_3)$	$T_{\text{pc}}(\text{Na}_3\text{AlF}_6)$ [°C]	$T_{\text{pc}}(\text{Na}_2\text{SiO}_3)$ [°C]	T_{eut} [°C]
0.000	1008	–	–
0.005	1007	–	–
0.020	1006	–	–
0.025	1003	–	881
0.035	1001	–	883
0.050	999	–	884
0.100	989	–	887
0.200	971	–	887
0.250	960	–	886
0.300	949	–	887
0.350	931	–	886
0.375	918	–	887
0.400	906	–	887
0.420	894	–	886
0.445	886	–	–
0.470	–	891	886
0.485	–	899	886
0.500	–	908	885
0.600	–	960	885

Cryoscopy can be a useful technique for the study of chemical reactions taking place in the melts between components. For the lowering of the fusion temperature of the solvent A, $\delta_{\text{fus}}T(\text{A})$, caused by the addition of the solute B, Eqn. 1 holds true, where R is the gas constant, $T_{\text{fus,A}}$ and $\Delta_{\text{fus}}H_{\text{A}}$ are the temperature and enthalpy of fusion of the solvent A, respectively, x_{B} is the mol fraction of the solute B, and k_{St} is the semi-empirical correction factor introduced by *Stortenbeker* [3], representing the number of foreign particles which are introduced by the solute B into the solvent A. By differentiating Eqn. 1 according to x_{A} and setting for $x_{\text{A}} \rightarrow 1$, Eqn. 2 is obtained for the tangent k_0 to the liquidus curve of the solvent A at the temperature of fusion of the solvent A.

$$\delta_{\text{fus}}T(\text{A}) = \frac{RT_{\text{fus,A}}^2}{\Delta_{\text{fus}}H_{\text{A}}} x_{\text{B}} k_{\text{St}} \quad (1)$$

$$\lim_{x_{\text{A}} \rightarrow 1} \frac{d(\delta_{\text{fus}}T(\text{A}))}{dx_{\text{A}}} = \frac{RT_{\text{fus,A}}^2}{\Delta_{\text{fus}}H_{\text{A}}} k_{\text{St}} = k_0 \quad (2)$$

The *Stortenbeker* correction factor, k_{St} , can be calculated from the tangent k_0 when $T_{\text{fus,A}}$ and $\Delta_{\text{fus}}H_{\text{A}}$ are known. The k_{St} value enables one to elucidate the possible chemical reactions between the components. In the case of our system, the value of the *Stortenbeker* correction factor was calculated from the tangent of the experimental liquidus curve of cryolite (Na_3AlF_6) at the melting point of pure Na_3AlF_6 (1281 K) according to Eqn. 2. For the enthalpy of fusion of Na_3AlF_6 , the calorimetrically determined value $\Delta_{\text{fus}}H_{\text{Na}_3\text{AlF}_6} = 106.75 \text{ kJ mol}^{-1}$ was used [4]. The dependence of ΔT_{PC}

on $x_{\text{Na}_3\text{AlF}_6}$ was expressed in the form of the linear regression $\Delta T_{\text{PC}} = (190.4 \pm 1.7) - (109.4 \pm 1.8) x_{\text{Na}_3\text{AlF}_6}$. For the constant of thermal depression, $RT_{\text{fus,A}}^2 / \Delta_{\text{fus}} H_{\text{A}}$, the value 127.80 K was obtained. For k_0 and k_{St} , the values $k_0 = 190.4$ K and $k_{\text{St}} = 1.5$ were then calculated. From *Stortenbecker's* concept it follows that 1 mol of Na_2SiO_3 introduced into an infinite amount of cryolite will produce 1.5 mol of reaction products, excluding the dissociation products of pure cryolite [5].

The phase diagram of the investigated part of the $\text{Na}_3\text{AlF}_6/\text{Na}_2\text{SiO}_3$ system is shown in *Fig. 1*. The diagram contains two quasi-eutectic points. The coordinates of these points are 42.8 mol-% of Na_2SiO_3 and 886°, 46.3 mol-% of Na_2SiO_3 and 886°, respectively. Between these two points, a region of two immiscible liquids was assumed. The effect of immiscibility of two liquids is often spotted in glass silicate melts [6]. Examination of the cooled sample cakes after the thermal analyses confirmed this assumption. The sample cake obtained from cryolite/44.5 mol-% of Na_2SiO_3 was easily mechanically separated in two fractions having the same color but different hardness. IR Spectroscopy and X-ray diffraction were used for the structural analysis of these layers (see below).

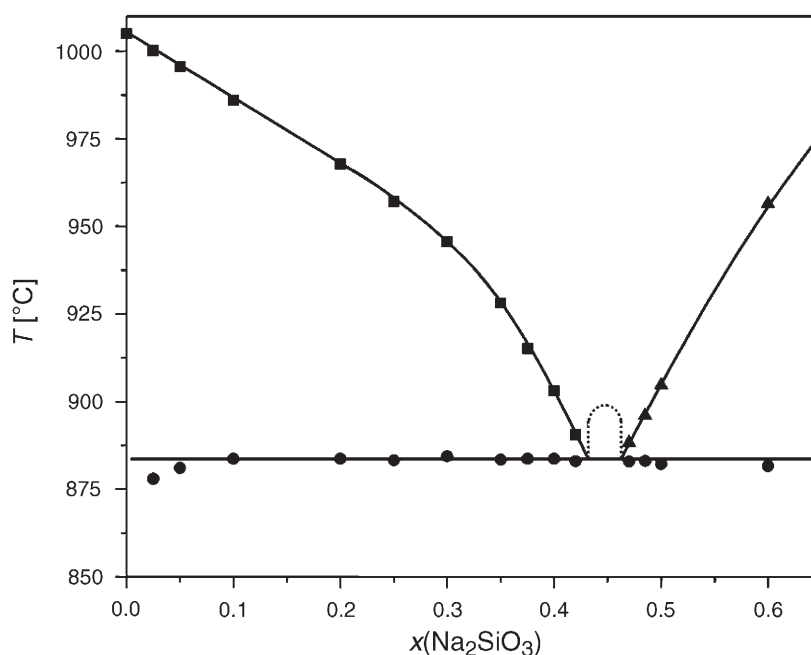


Fig. 1. Phase diagram of the system $\text{Na}_3\text{AlF}_6/\text{Na}_2\text{SiO}_3$

As an example of the thermal-analysis measurements, the cooling curve of the system with 2.5 mol-% of Na_2SiO_3 was selected (*Fig. 2*). Two thermal effects were clearly revealed by the curve; the first one corresponds to the primary crystallization (around 1000°C), and the second one to the eutectic crystallization (around 878°C). A small undercooling at both thermal effects is observed (*ca.* 3–4°C). This behavior is typical for molten silicates that do not crystallize easily [6]. This reluctance is the

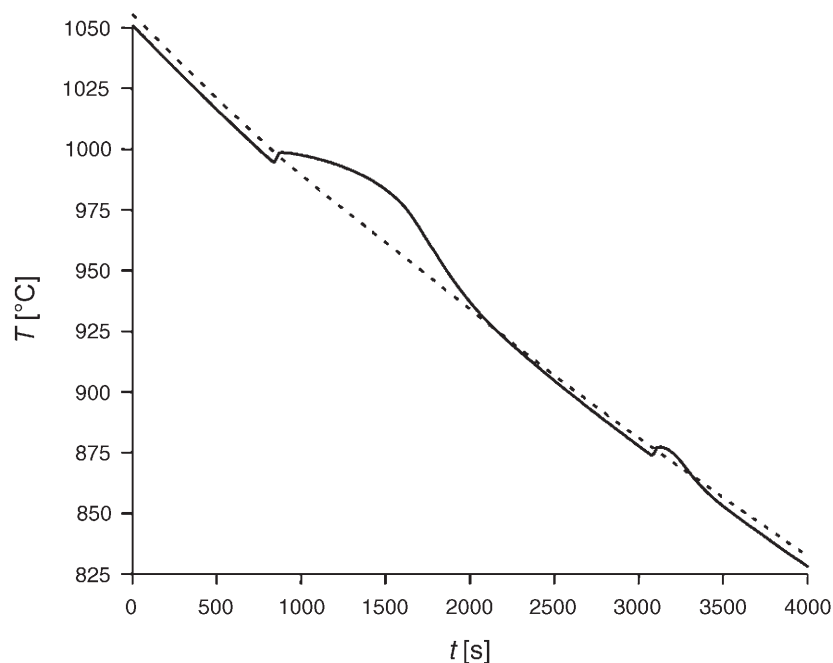


Fig. 2. Cooling curve of the system $\text{Na}_3\text{AlF}_6/2.5$ mol-% of Na_2SiO_3 . Solid line, measured thermocouple; dashed line, reference thermocouple.

consequence of the tendency of polysilicate ions to form large clusters of the $\{\text{SiO}_4\}$ tetrahedra variously connected into the multiplex structures.

2.2. Mass-Loss Analysis. The mass losses of investigated mixtures measured during 1 h at 1020°C are summarized in *Table 2*. The one-hour mass loss Δm of pure cryolite at 1020°C was found to be 10.8%. It is well known that cryolite undergoes substantial thermal dissociation at melting through the formation of volatile NaAlF_4 and NaF that remain in the bulk [7].

As can be seen from *Table 2*, the one-hour mass losses Δm of melts slightly decrease with increasing content of Na_2SiO_3 as compared to pure cryolite. This is caused by the

Table 2. Mass Losses (Δm) in the System $\text{Na}_3\text{AlF}_6/x$ mol-% of Na_2SiO_3 ($x = 0, 10, 20, 40$ and 60) at 1020°C after 1 h

Mass m of sample [mg]	Sample	Δm (1020°), 1 h	
		[mg]	mass-%
300	blank	– 2.0	0.7
300	Na_3AlF_6	– 32.3	10.8
300	10 mol-% of Na_2SiO_3	– 17.5	5.8
300	20 mol-% of Na_2SiO_3	– 17.6	5.8
300	40 mol-% of Na_2SiO_3	– 11.8	3.9
300	60 mol-% of Na_2SiO_3	– 9.7	3.2

decreasing amount of cryolite in the melts producing less volatile NaAlF_4 . From these experimentally determined mass losses follows that Na_2SiO_3 reacts with cryolite under the formation of nonvolatile products.

2.3. *X-Ray-Diffraction and IR Analysis.* X-Ray diffraction was performed with the samples after thermal analyses. As one can see from Fig. 3, all analyzed samples (cryolite + 30, 40, and 50 mol-% of Na_2SiO_3) exhibit only two crystalline phases, cryolite and NaF, respectively. The intensity of the cryolite diffractions decreases with decreasing content of cryolite. Diffraction patterns of samples containing Na_2SiO_3 exhibit new diffractions at 45.40° and 66.25° (2θ), that belong to NaF. The intensity of the NaF diffractions increases with increasing content of Na_2SiO_3 . Based on this observation, it can be concluded that the formed NaF does not originate from the dissociation reaction of cryolite but is formed as the reaction product of cryolite and Na_2SiO_3 . The absence of diffractions of other expected products can have two reasons. Either such a product escaped from the system as volatile compound or it was present but in the noncrystalline form. The first assumption can be excluded by means of the mass-loss analyses (see above). The second assumption is verified by the observation of slight background signals in the range from 15° to 40° (2θ) of the diffraction plots. This background feature is typical for glassy phases. In the case of systems containing aluminium and silicon oxides, the formation of vitreous alumino-silicates is commonly observed.

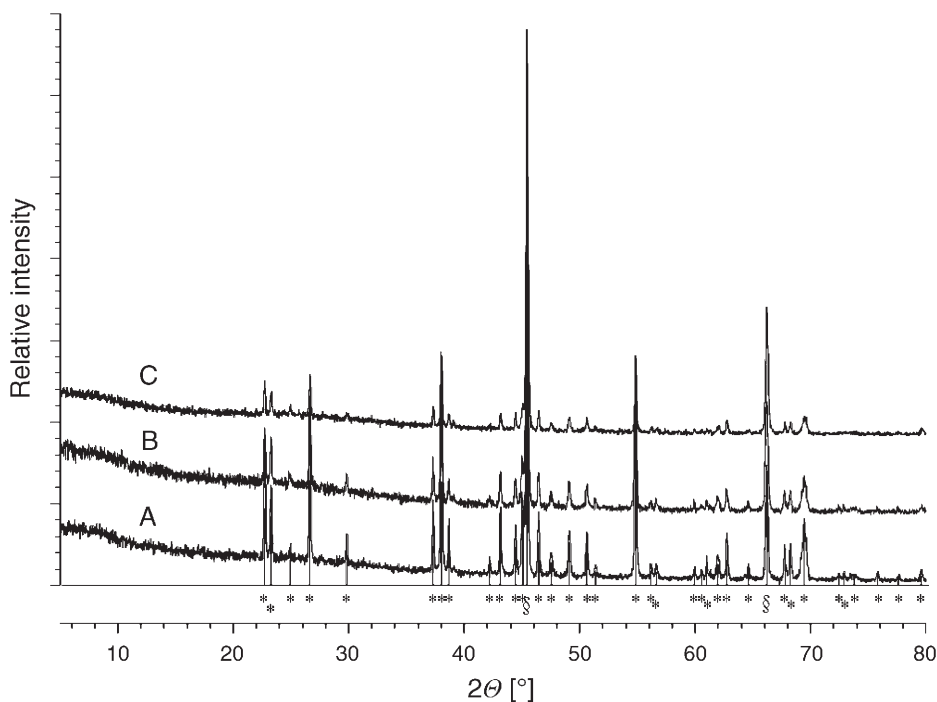


Fig. 3. Comparison of the X-ray-diffraction plots of solidified samples with different content of Na_2SiO_3 . A, 30 mol-%, B, 40 mol-%, C, 50 mol-%; *, Na_3AlF_6 ; §, NaF.

The middle IR spectra ($400\text{--}2000\text{ cm}^{-1}$) of spontaneously cooled products with an Na_2SiO_3 content of up to 50 mol-% contain all a band with a maximum at 600 cm^{-1} that is characteristic for AlF_6^{3-} in cryolite [8][9] (Fig. 4). Compared with pure cryolite, the spectra of $\text{Na}_3\text{AlF}_6/\text{Na}_2\text{SiO}_3$ samples have several new bands: a strong broad band at 1018 cm^{-1} , two weak shoulders at 800 and around $750\text{--}700\text{ cm}^{-1}$, and a shoulder at 470 cm^{-1} . The positions of these bands are similar to those of the dominant vibrations in amorphous silica (stretching at 1105 cm^{-1} , bending at 800 cm^{-1} , and rocking at 470 cm^{-1}) [10]. Therefore, it can be assumed that in the investigated systems, a polymeric tetrahedral aluminosilicate network originates from the reaction between cryolite and Na_2SiO_3 . The aluminosilicate spectra resemble the silica one with three main bands, but their position depends on the $\text{Al}^{\text{IV}}/\text{Si}^{\text{IV}}$ ratio. The similarities are due to the geometrical equivalence of the aluminosilicate network to the silica network, while differences are due to different chemical bonds. The Si–O–Si bridges present in SiO_2 are substituted in the system $\text{Na}_3\text{AlF}_6/\text{Na}_2\text{SiO}_3$ by the Si–O–Al bridges. The strongest complex band in the range $900\text{--}1200\text{ cm}^{-1}$ should be assigned to two types of the stretching vibrations. The wavenumber around 1100 cm^{-1} is due to Si–O(Si) (the atom in the parentheses denotes the closest atom bonded to the O-atom) and the wavenumber around 1000 cm^{-1} to the Si–O(Al) stretching modes. The shoulder at 800 cm^{-1} belongs to the bending Si–O–Si vibration, while a new band in the range of

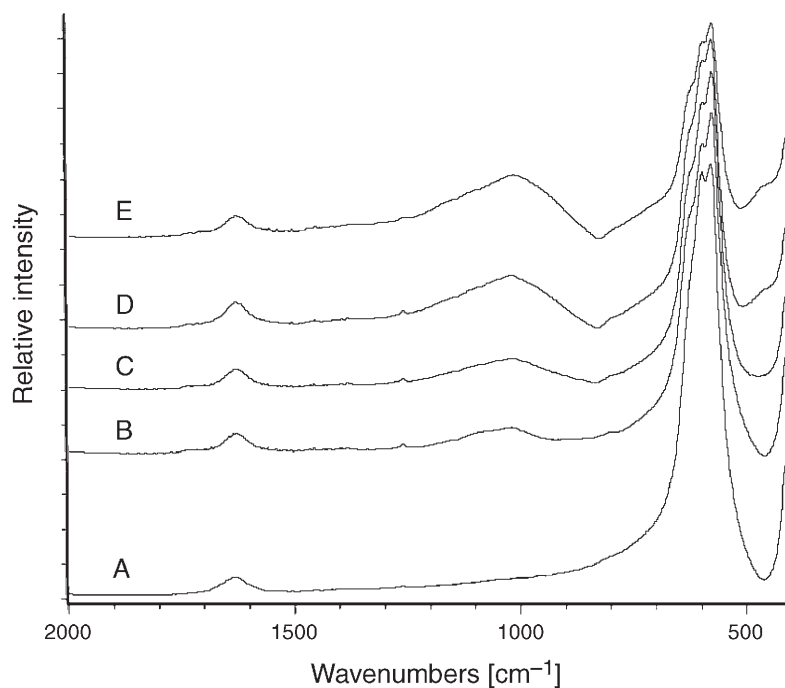


Fig. 4. IR Spectra of the solidified samples of the systems $\text{Na}_3\text{AlF}_6/x$ mol-% of Na_2SiO_3 ($x = 10, 30, 40$ and 50), spontaneously cooled from 1050° . A, pure Na_3AlF_6 ; B, 10 mol-% of Na_2SiO_3 ; C, 30 mol-% of Na_2SiO_3 ; D, 40 mol-% of Na_2SiO_3 ; E, 50 mol-% of Na_2SiO_3 .

730–700 cm^{-1} is due to new Al–O(Si) stretching modes [11][12]. The last band at 470 cm^{-1} is assigned to a rocking motion of the O-atom in the Si–O–Si units.

The IR spectra of the two immiscible separate layers (see above) obtained from a cryolite/44.5 mol-% of Na_2SiO_3 sample after the thermal analysis confirm the assumptions mentioned above (Fig. 5). The mechanically harder layer (A in Fig. 5) mainly contains the polymeric aluminosilicate compounds. The strongest complex band is the product of the overlapping Si–O(Si) stretching vibrations at 1100 cm^{-1} and Si–O(Al) vibrations at 1020 cm^{-1} . The Si–O(Al) vibrations generally appear in the range 900–1040 cm^{-1} depending on the $\text{Al}^{\text{IV}}/\text{Si}^{\text{IV}}$ ratio: the higher the ratio, the lower energies are achieved. The band in the range 700–800 cm^{-1} with a maximum at 703 cm^{-1} is the product of the overlapping Si–O–Si bending vibration and Al–O(Si) stretching modes. The maximum at 703 cm^{-1} clearly confirms the presence of new Al–O bonds in the formed aluminosilicates [10][13]. The weak band at 600 cm^{-1} is assigned to the Al–F vibrations of cryolite.

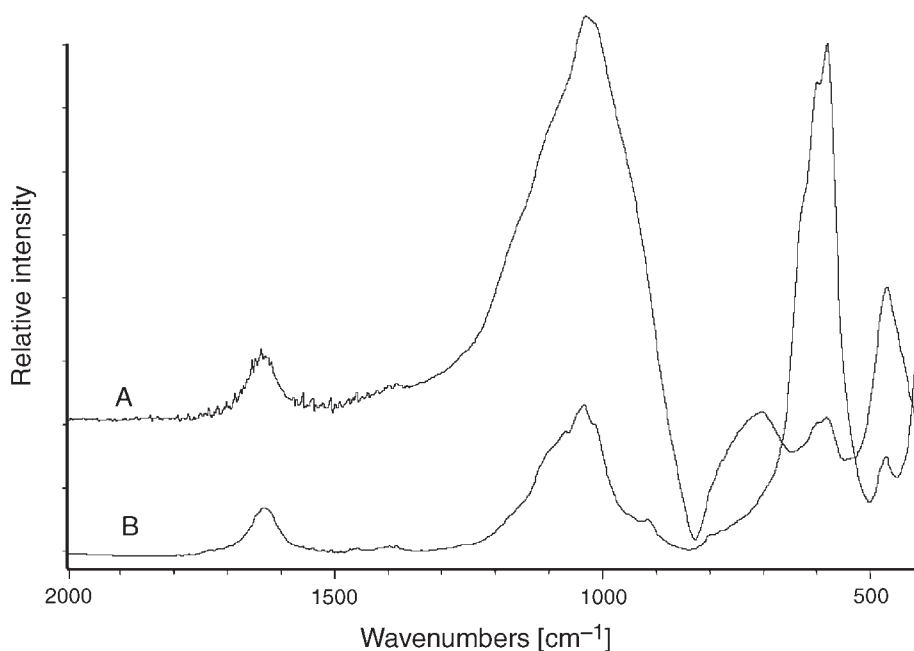


Fig. 5. Comparison of the IR spectra of the two layers obtained from spontaneously cooled samples containing 44.5 mol-% of Na_2SiO_3 . A, lower, mechanically harder layer; B, upper, mechanically softer layer.

The mechanically softer layer (B in Fig. 5) mainly exhibits the vibration of pure cryolite at 600 cm^{-1} . The other bands belong to vibrations of the new aluminosilicate network as it was mentioned above. As one can see from Fig. 5, the separation of the two phases is not complete, a fact that also follows from the theory of immiscibility [14]. NaF is not observed in the investigated range of the IR spectra.

3. Conclusions. – The phase analysis between cryolite and sodium metasilicate was experimentally examined by thermal analysis. The simple eutectic system with a region of two immiscible substances arising in a 42.8–46.3 mol-% concentration range of Na_2SiO_3 was observed. From the results of the cryoscopic calculation, it follows that the number of the new species is 1.5. It indicates that 1 mol of Na_2SiO_3 introduced into the infinite amount of cryolite will produce 1.5 mol of reaction products, excluding the dissociation products of pure cryolite. Based on the mass losses of the investigated mixtures, it can be concluded that Na_2SiO_3 reacts with cryolite under the formation of nonvolatile products. The IR and X-ray analyses of the solidified samples indicate the formation of NaF and the stable vitreous alumino-silicate network.

This work was supported by the *Slovak Grant Agency VEGA 2/7077/27* and by the *Science and Technology Assistance Agency* under contract No. APVV-51-008104.

Experimental Part

General. For the preparation of the samples, the following chemicals were used: NaF (*Merck*; 99.5%), AlF_3 (sublimated, dried at 300 °C; min. 99.0%), Na_2SiO_3 (*Aldrich*; 99.5%), cryolite (Norwegian, hand picked), NaCl (*Fluka*; 99.5%). Handling of all salts was performed in a glove box under the dry inert nitrogen atmosphere (*Messer*; 99.990%). All measurements were performed under Ar (*Messer*; 99.996%).

Thermal Analysis. The thermal effects were studied in the mixtures NaF/ AlF_3 at the cryolite composition containing Na_2SiO_3 in a range $0 < x(\text{Na}_2\text{SiO}_3) < 0.6$. Then 10.0000 ± 0.0002 g of the homogenized mixtures was placed in a Pt crucible. The crucible with sample was heated in a resistance furnace. Heating curves were recorded up to 50 °C over the complete melting of the mixture, with a heating rate of ca. 7 °C min⁻¹. Then, the cooling curves were recorded as well; however, the cooling rate did not exceed 2 °C min⁻¹. The temp. of the mixtures were measured with a Pt/Pt10Rh thermocouple immersed directly into the melt. The thermocouple was calibrated to the melting point of pure NaCl and NaF (the error of temp. of the thermocouple was determined to be +3 °C). The reproducibility of the measured temp. was within ±2 °C.

Mass-Loss Measurements. Thermogravimetric analysis was carried out with a derivatograph *Q-1500D*. Mass loss of samples of the composition $\text{Na}_3\text{AlF}_6/x$ mol-% of Na_2SiO_3 ($x = 0, 10, 20, 40, 60$), each weighing 300.0 ± 0.2 mg, were recorded. The samples were heated from r.t. up to 1020 °C. After reaching the final temp., the samples were kept at constant temp. for 1 h. The heating rates were 8–9 °C min⁻¹.

X-Ray Measurements. All samples were grounded to fine powders. The X-ray diffraction patterns were collected within the range 10–80° in steps of 0.02° (2θ) by using $\text{CoK}_{\alpha 1}$ radiation. The samples were mounted on the foils. To collect the X-ray patterns, a transmission *Stoe-Stadi-P* diffractometer equipped with a linear PSD and a curved Ge(111) primary beam monochromator was used.

Infrared Spectroscopy. The FT-IR spectra were obtained with a *Nicolet-Magna-750* spectrometer. In the middle-IR (MIR) region, a DTGS detector and KBr beam splitter were used. The spectra of each pressed KBr disk (1 mg of sample and 200 mg of KBr) were recorded from 128 scans with a resolution of 4 cm⁻¹.

REFERENCES

- [1] K. Grjotheim, C. Krohn, M. Malinovský, K. Matiašovský, J. Thonstad, 'Aluminium Electrolysis. Fundamentals of the Hall-Héroult Process', 2nd edn. Aluminium Verlag, Düsseldorf, 1982.
- [2] Å. Sterten, P. A. Solli, E. Skybakmoen, *J. Appl. Electrochem.* **1998**, 28, 781.
- [3] W. Stortenbeker, *Z. Phys. Chem.* **1892**, 10, 183.
- [4] Å. Sterten, I. Mæland, *Acta Chem. Scand.* **1985**, 39, 241.
- [5] I. Proks, V. Daněk, M. Chrenková, F. Šimko, Z. Pánek, *Chemical Papers* **2002**, 56, 71.

- [6] R. Smoluchowski, J. E. Mayer, W. A. Weyl, 'Phase Transformations in Solids', 2nd edn., John Wiley & Sons, Inc., New York, 1957.
- [7] M. Bruno, O. Herstad, J. L. Holm, *Acta Chem. Scand.* **1998**, 52, 1399.
- [8] A. de Lattre, *J. Chem. Phys.* **1951**, 19, 1610.
- [9] M. Globelny, *J. Fluorine Chem.* **1976**, 8, 353.
- [10] V. C. Farmer, A. R. Fraser, J. M. Tait, *Geochim. Cosmochim. Acta* **1979**, 43, 1417.
- [11] M. Handke, W. Mozgawa, *Vib. Spectrosc.* **1993**, 5, 75.
- [12] P. Tarte, *Spectrochim. Acta, Part A* **1967**, 23, 2127.
- [13] V. C. Farmer, G. S. R. Krishnamurti, P. M. Huang, *Clays Clay Miner.* **1991**, 39, 561.
- [14] B. Predel, M. Hoch, M. Pool, 'Phase Diagrams and Heterogeneous Equilibria', Springer Verlag, Germany, 2004.

Received February 26, 2007